

Fig. S1 | vTR and CoV activation screen details and validation, related to Figure 1. (A) Detailed schematic of the HT-Recruit dual reporter cassette when integrated into the *AAVS1* locus in the first intron of the *PPP1R12C* gene. puroR = puromycin resistance, polyA = polyadenine tail, TetO = tetracycline operator sequence, IgK leader = immunoglobulin K signaling sequence for secretion, IgG-Fc = immunoglobulin G constant region. **(B)** Flow cytometry distributions on day two of recruitment for replicate screen minCMV reporter cells before and after magnetic separation. **(C)** Example flow cytometry distributions without (no dox, gray) and with (dox, yellow) two days of recruitment for individually validated activator tiles from human adenovirus 9 (HAdV9) E1A and herpes simplex virus 1 (HSV1) VP16. The percentages of the dox-treated cells that are mCitrine-negative (OFF) and mCitrine-positive (ON) are indicated to the left and right, respectively, of the dashed line. **(D)** Summary of activation strengths of individually validated tiles as assessed by flow cytometry (no dox in gray, dox in yellow). Tiles are ranked by screen score, with percent of ON cells shown on the x-axis. **(E)** Relationship between activation $\log_2(\text{ON}:\text{OFF})$ enrichment score from the screen and the percent of ON cells for the set of individually validated tiles in (D). Logistic fit in gray with Spearman $r = 0.86$. The gray dashed line at $x = 3.25$ represents the detection threshold. **(F)** Flow cytometry distributions on day five of recruitment for replicate screen pEF reporter cells before and after magnetic separation. **(G)** Example flow cytometry distributions without (no dox, gray) and with (dox, blue) five days of recruitment for individually validated repressor tiles from human cytomegalovirus (HCMV) IE2 and HAdV40 E1A. **(H)** Summary of repression strengths of individually validated tiles as assessed by flow cytometry (no dox in gray, dox in blue). Tiles are ranked by screen score, with percent of OFF cells shown on the x-axis. **(I)** Relationship between repression $\log_2(\text{OFF}:\text{ON})$ enrichment score from the screen and the percent of OFF cells for the set of individually validated tiles in (H). Logistic fit in gray with Spearman $r = 0.92$. The gray dashed line at $x = 0.69$ represents the detection threshold. **(J-L)** Tiling plots for three VP16 homologs included in the vTR library: HSV1 VP16 (J), HSV2 VP16 (K), and varicella zoster virus (VZV) VP16 (L). Activation and repression domains are highlighted as vertical spans. **(M-O)** Tiling plots for three E1A homologs included in the vTR library: HAdV5 E1A (M), HAdV9 E1A (N), HAdV40 (O). **(P)** Activation screen reproducibility plot as in Fig. 1C, but rendered as contours and colored by virus genome type (DNA or RNA). **(Q)** Repression screen reproducibility plot as in Fig. 1D, but rendered as contours and colored by virus genome type.

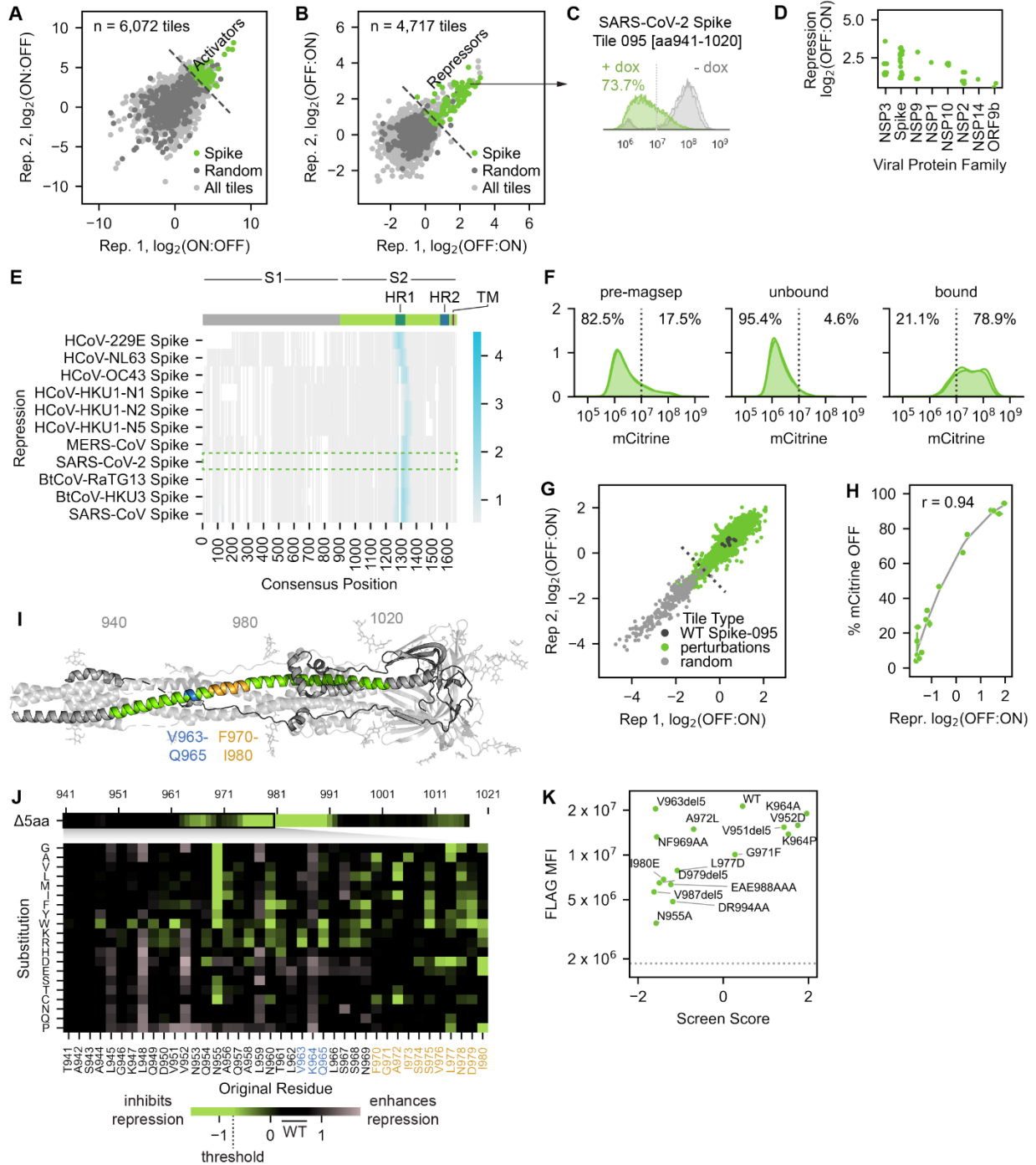


Fig. S2 | Coronavirus Spike proteins contain a functionally conserved region with transcriptional repression potential, related to Figure 1. (A-B) Coronavirus screen reproducibility plots for activation (A) and repression (B), with tiles from Spike protein homologs indicated. **(C)** Flow cytometry distributions without (no dox, gray) and with (dox, green) recruitment of the SARS-CoV-2 Spike tile 095 (Spike-095) to the pEF reporter after 5 days. **(D)** Summary of identified repression domains, represented by their strongest tile and stratified by viral protein family. **(E)** Top: schematic of a typical coronavirus Spike protein, with the S1 and S2 fragments, heptad repeat (HR) 1 and 2 regions, and transmembrane (TM) portion indicated. Bottom: multiple

sequence alignment of 11 coronavirus Spike homologs with repression domains indicated. Repression $\log_2(\text{OFF}:\text{ON})$ enrichment scores are represented as blue color mappings. The SARS-CoV-2 Spike homolog is outlined in a green box, and its Spike-095 tile from (C) overlaps HR1. (F) To understand the physical basis for Spike-095 transcriptional repression, we designed a library comprising natural and systematically mutated Spike-095 variants and performed HT-recruit as before. Shown here are flow cytometry distributions on day seven of recruitment for replicate screen pEF reporter cells before and after magnetic separation. (G) Spike-095 perturbation screen reproducibility plot, showing repression $\log_2(\text{OFF}:\text{ON})$ enrichment scores across two replicates. The detection threshold (dashed line) is set as two standard deviations above the mean of the random negative controls and is equal to -0.73. (H) Relationship between repression $\log_2(\text{OFF}:\text{ON})$ enrichment score from the screen and the percent of mCitrine-negative (OFF) cells for a set of individually validated tiles as assessed by flow cytometry. Logistic fit in gray with Spearman $r = 0.94$. (I) Structure of the SARS-CoV-2 Spike S2 fragment in the natural trimeric complex (PDB: 6XRA) that forms after entry and cleavage by host proteins. Spike-095 is indicated in green for one monomer, with other regions of interest in the perturbation screen indicated in blue and orange. (J) Heatmaps of perturbation screen results. Average screen scores for overlapping 5aa deletions within the region of residues 941-1020 are shown on top, with the most important residues for function being 960-990. Screen scores for each substitution within the 'core' region (residues 941-980, representing the intersection of all repressive tiles within the SARS-CoV-2 repression domain) are shown below. Biochemically dissimilar substitutions within residues 977-981 are generally detrimental to silencing, especially for normally inward-facing non-polar residues L977 and I980, with no substitutions enhancing activity. In contrast, a number of substitutions outside this region actually enhance silencing. These include non-polar residues L945, L948, V952, or L959, which would normally contribute to stabilizing hydrophobic interactions at the Spike trimerization interface. Enhanced silencing is also observed when almost any residue from 945-964 is substituted to proline, which is known to disrupt alpha helices like that which is predicted for the Spike-095 tile. Taken together, Spike-095 may transition between a homotrimeric state to a monomeric state where residues L977 and I980 are available to interact with leucine zippers in co-repressors. (K) Fusion protein levels (rTetR-3xFLAG-effector) are estimated using anti-FLAG staining and flow cytometry. Scatterplot of screen score against FLAG MFI (proxy for protein levels). Dashed line represents background FLAG staining signal from WT cells (no protein expression), showing all mutants are expressed, albeit at different levels, regardless of their screen score.

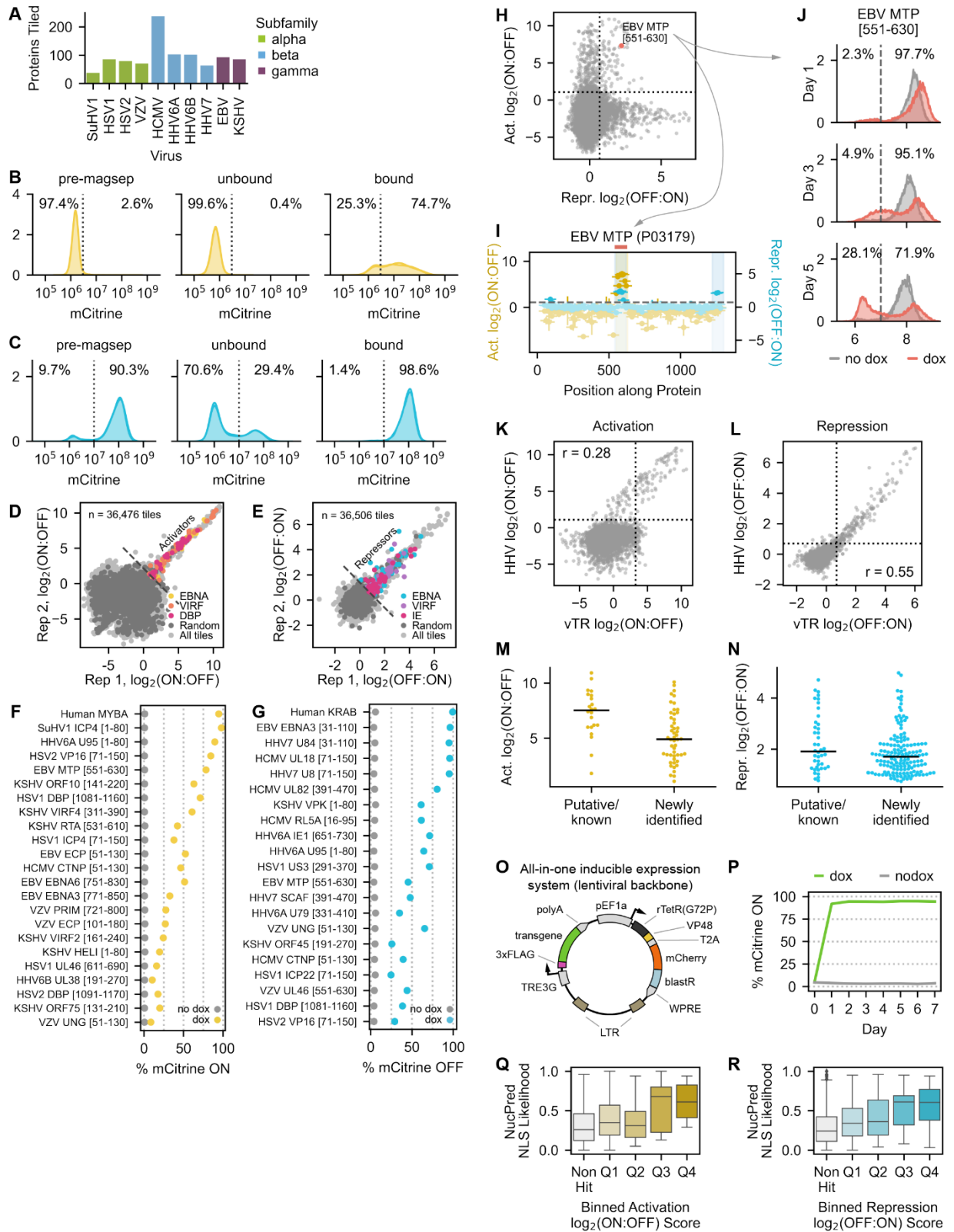


Fig. S3 | Herpesvirus tiling screen details and validations, related to Figure 2. (A) Summary of the number of proteins tiled for each herpesvirus species, colored by subfamily. Tiled proteins were pulled from UniRef90 and represent nearly complete proteome coverage. (B-C) Flow cytometry distributions on day two of recruitment for replicate screen minCMV reporter cells (B) and on day five of recruitment for replicate screen pEF reporter cells (C) before and after magnetic separation. (D) Reproducibility of activation $\log_2(\text{ON}:\text{OFF})$ enrichment scores across two replicates, with hit tiles from EBNA, VIRF, and DBP proteins (investigated later) indicated. The gray dashed line represents the detection threshold, which is 1.08. (E) Reproducibility of repression $\log_2(\text{OFF}:\text{ON})$ enrichment scores across two replicates, with hit tiles from EBNA, VIRF, and IE proteins (former two investigated later) indicated. The gray dashed line represents the detection threshold, which is 0.70. (F) Summary of activation strengths of individually validated tiles as assessed by flow cytometry (no dox in gray, dox in yellow). Tiles are ranked by screen score, with percent of mCitrine-positive (ON) cells shown on the y-axis. (G) Summary of repression strengths of individually validated tiles as assessed by flow cytometry (no dox in gray, dox in blue). Tiles are ranked by screen score, with percent of mCitrine-negative (OFF) cells shown on the y-axis. (H) Activation versus repression screen scores. Tiles with dual activities are in the top right quadrant. One example from EBV MTP is highlighted in red. (I) Tiling plot of EBV MTP with its dual effector domain highlighted with a red bar. This domain displays strong activation and moderate repression potential. (J) Gene silencing dynamics of the dual effector tile from EBV MTP highlighted in (H) upon recruitment at the pEF reporter: mCitrine levels initially increase in all cells, then subsequently bifurcate, with one population maintaining elevated mCitrine levels relative to the no dox sample and the other silencing completely by day 5 of recruitment. These dynamics are observed for several validated dual effector tiles (data not shown) and are similar to those observed for a set of dual effectors tiles from human transcription factors, albeit at a different promoter²⁵. (K-L) Scatterplot of the average activation (K) or repression (L) screen scores for tiles shared between the vTR and herpesvirus (HHV) libraries. (M-N) Comparison of activation (M) and repression (N) domain strengths for putative/known herpesvirus effector proteins present in both the vTR and HHV tiling screens versus those newly identified in the HHV tiling screen. (O) Plasmid design for all-in-one inducible expression of full-length viral proteins on a third generation lentiviral backbone. The pEF1a promoter constitutively expresses a non-leaky reverse tetracycline repressor (rTetR(G72P) mutant) fused to the strong activation VP48 domain, which, upon doxycycline (dox) addition, can activate the TRE3G promoter for expression of a transgene: either a full-length viral protein or mCitrine as a negative control. The rTetR(G72P)-VP48 is linked by a ribosome-skipping T2A sequence to a fusion protein of mCherry and an enzyme conferring resistance to blasticidin (blastR) for visualization and selection purposes. (P) Time course showing sustained, robust expression of an mCitrine transgene with the system described in (O) with continued doxycycline treatment. (Q-R) Boxplots of predicted NLS (NucPred score) across full-length viral proteins, binned by activation (Q) or repression (R) screen score of their effector domains. Q1 through Q4 represent the first through fourth quartiles of effector strength.

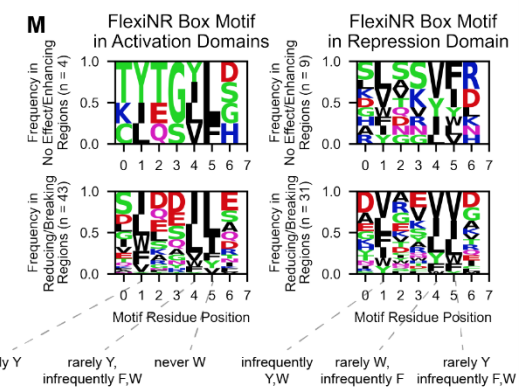
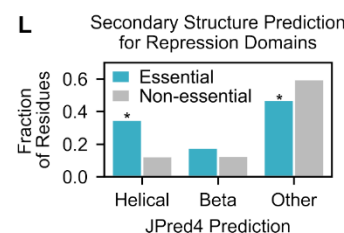
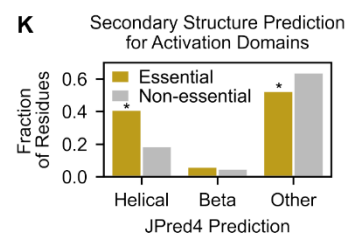
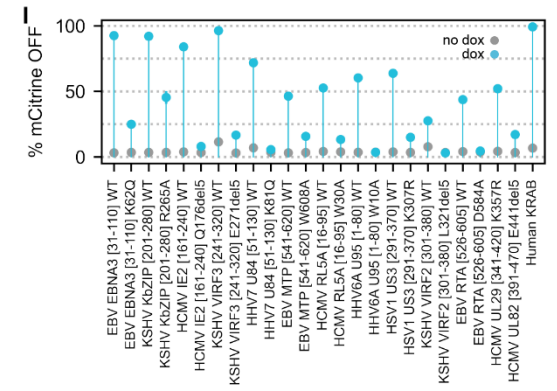
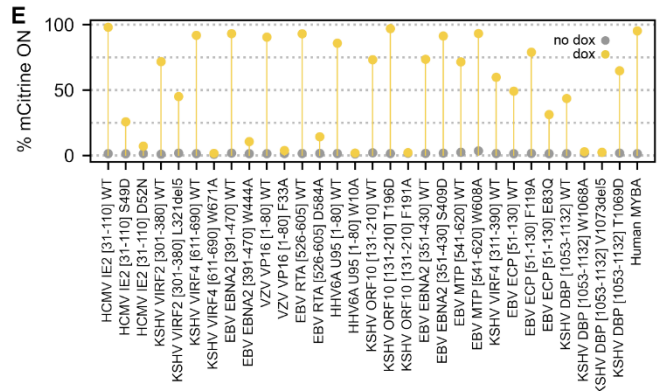
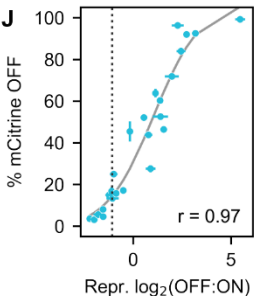
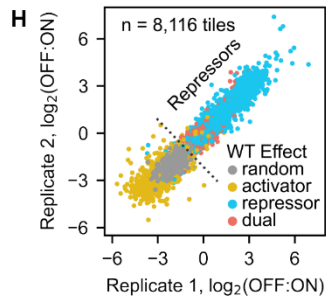
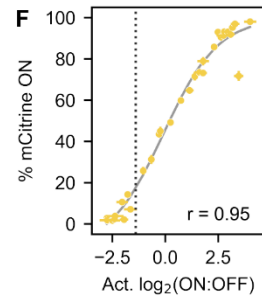
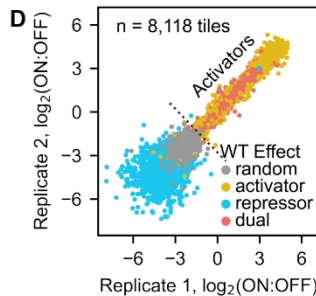
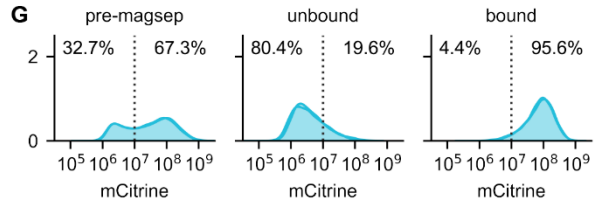
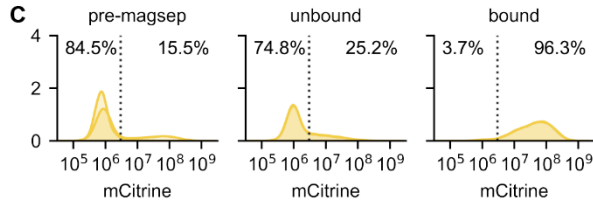
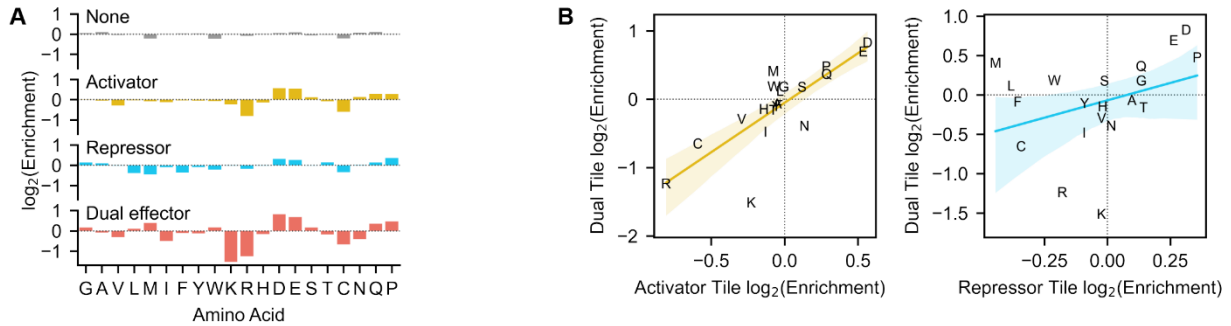


Fig. S4 | Herpesvirus sequence features and perturbation screen details and validation, related to Figure 3. (A) Barplots of the log₂-transformed ratios of amino acid frequencies in tiles with no activity (gray, top row), activation (yellow, second row), repression (blue, third row), and dual effector (red, bottom row) tiles relative to their proteome frequencies. Positive values represent an enrichment in effector domains while negative values represent a depletion. (B) Comparison of the amino acid enrichments in (A) showing a stronger correlation between activator and dual effector tiles (left) than repressor and dual effector tiles (right). (C) Flow cytometry distributions on day two of recruitment for replicate screen minCMV reporter cells before and after magnetic separation. (D) Reproducibility of activation log₂(ON:OFF) enrichment scores across two replicates, with each tile colored according to its original effector category in the HHV tiling screen (random, activator, repressor, and dual effector). (E) Summary of activation strengths of individually validated tiles as assessed by flow cytometry (no dox in gray, dox in yellow). Tiles are ranked by wild-type screen score, with percent of mCitrine-positive (ON) cells shown on the y-axis and the MFI of ON cells represented as marker size. (F) Relationship between activation log₂(ON:OFF) enrichment score from the screen and the percent of ON cells for the set of individually validated tiles in (E). Logistic fit in gray with Spearman $r = 0.95$. The gray dashed line at $x = -1.39$ represents the detection threshold. (G) Flow cytometry distributions on day five of recruitment for replicate screen pEF reporter cells before and after magnetic separation. (H) Reproducibility of repression log₂(OFF:ON) enrichment scores across two replicates. (I) Summary of repression strengths of individually validated tiles as assessed by flow cytometry (no dox in gray, dox in yellow). Tiles are ranked by wild-type screen score, with percent of mCitrine-negative (OFF) cells shown on the y-axis and the MFI of OFF cells represented as marker size. (J) Relationship between repression log₂(OFF:ON) enrichment score from the screen and the percent of OFF cells for the set of individually validated tiles in (H). Logistic fit in gray with Spearman $r = 0.97$. The gray dashed line at $x = -1.07$ represents the detection threshold. (K-L) Barplots comparing the fraction of residues within essential (colored) or non-essential regions (gray) regions in activation (K) or repression (L) domains that have a particular secondary structure as predicted by JPred4. (M) Logos showing the frequency of amino acids at each position of the flexiNR box motif for instances in regions whose deletion has no effect or enhances activity (top row) versus regions whose deletion reduces or breaks activity (bottom row) in activation (left) or repression (right) domains. The flexiNR motif used in this initial search was maximally flexible and was refined for subsequent analysis based on which amino acids rarely occurred at a given position (Methods). Negative charge and phosphorylatable residues (S/T) are common at the variable positions throughout this motif.

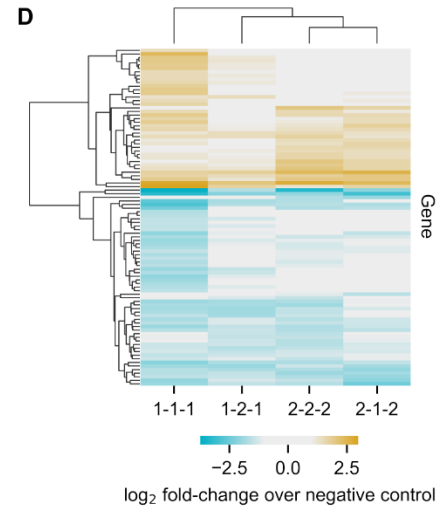
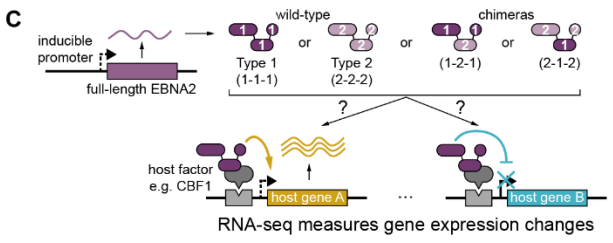
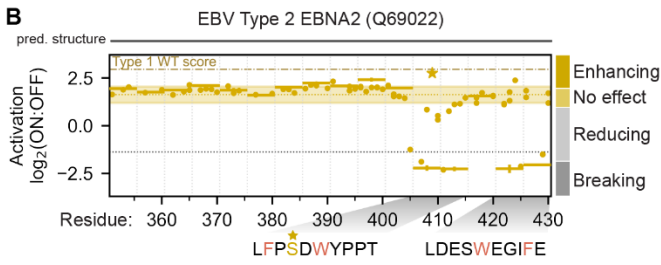
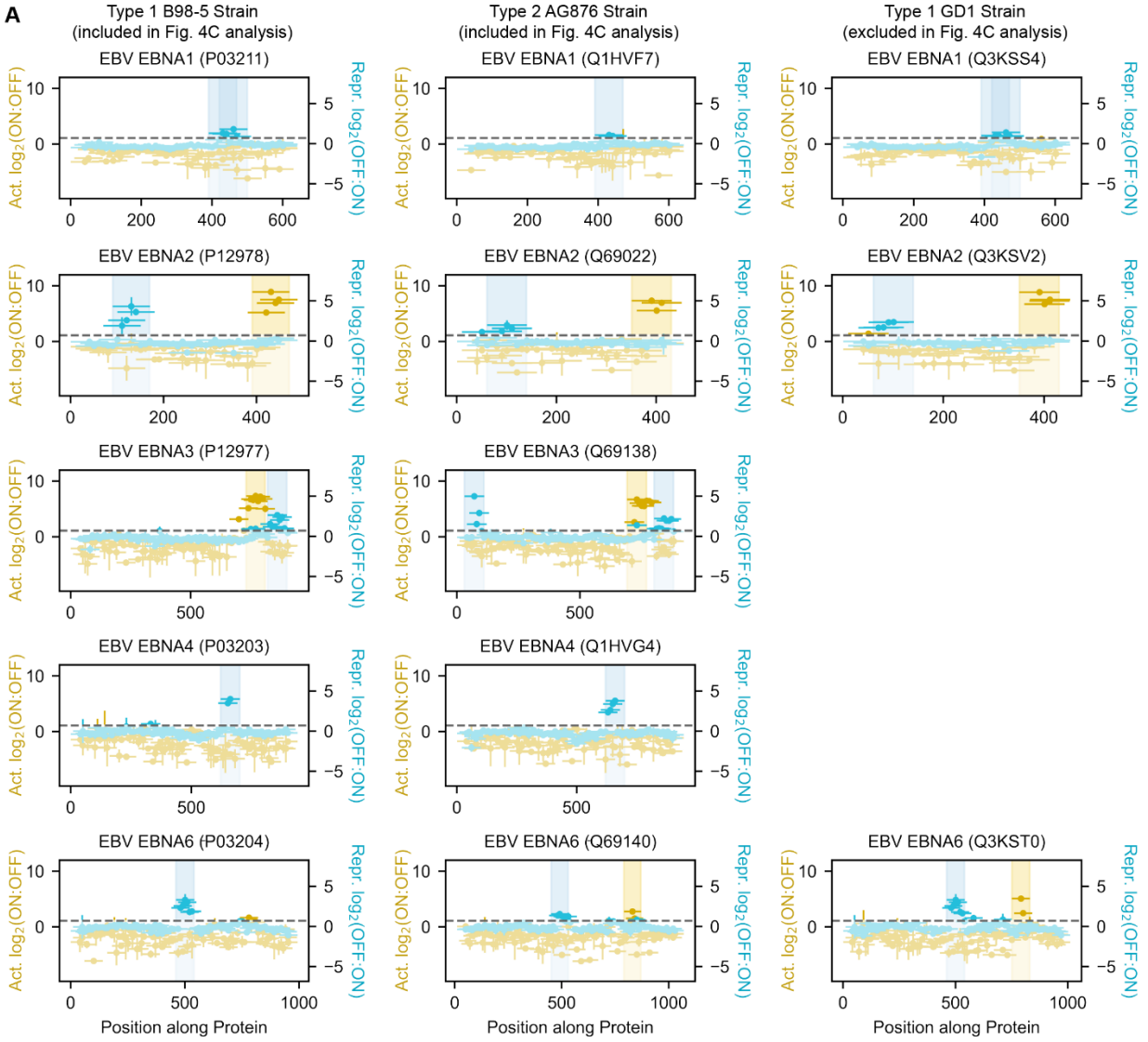


Fig. S5 | Effector domains across EBNA protein homologs, related to Figure 4. (A) Tiling plots for all EBNA proteins with effector domains identified in the HHV tiling library. Rows delineate EBNA protein types, while columns delineate EBV strains. EBV type 1 and type 2 are represented by the classical B95-8 and AG876 strains, respectively, which were used for the analysis in Fig. 4C and subsequent RNA-seq experiments. **(B)** Perturbation tiling plot mapping the effects of single-residue substitutions (dots) and 5aa deletions (horizontal spans) on the maximum-strength tiles from the activation domain of EBV type 2 EBNA2. JPred4-predicted secondary structure is shown above the plot, with straight lines indicating non-alpha helix and non-beta sheet regions (includes unstructured). The shaded horizontal span represents the wild-type screen score mean plus/minus two times the estimated error (mean of all wild-type tiles shown as the yellow horizontal dotted line within). Perturbations with scores within these regions are considered to have 'no effect', while those above and below are considered 'enhancing' and 'reducing', respectively. The gray horizontal dotted lines represent the detection thresholds, and thus perturbations whose scores are below this threshold are considered 'breaking'. Deleted regions below the detection threshold are deemed essential, and their sequences are displayed below the plot, with red residues indicating single-residue substitutions that abolish activity. The brown dotted-dashed line represents the type 1 EBNA2 WT screen score for comparison of activation strength, with the yellow star representing the S409D substitution that restores type 2 EBNA2 activation to that of its type 1 counterpart. **(C)** Full-length wild-type type 1 or type 2 EBNA2 (1-1-1 and 2-2-2) or chimeras with swapped effector domains (1-2-1 chimera with type 1 effector domains flanking the type 2 CBF1-binding domain and 2-1-2) are expressed in K562 cells from a dox-inducible promoter (Methods) to measure differential effects on host gene expression. **(D)** Cluster map of K562 genes that are differentially expressed in at least one EBNA2 wild-type or chimera overexpression condition, as measured by RNA-seq and presented as log-2 fold changes of significantly up- or downregulated genes relative to an mCitrine-expressing negative control. Sample abbreviations reflect those shown in the schematic in (C).

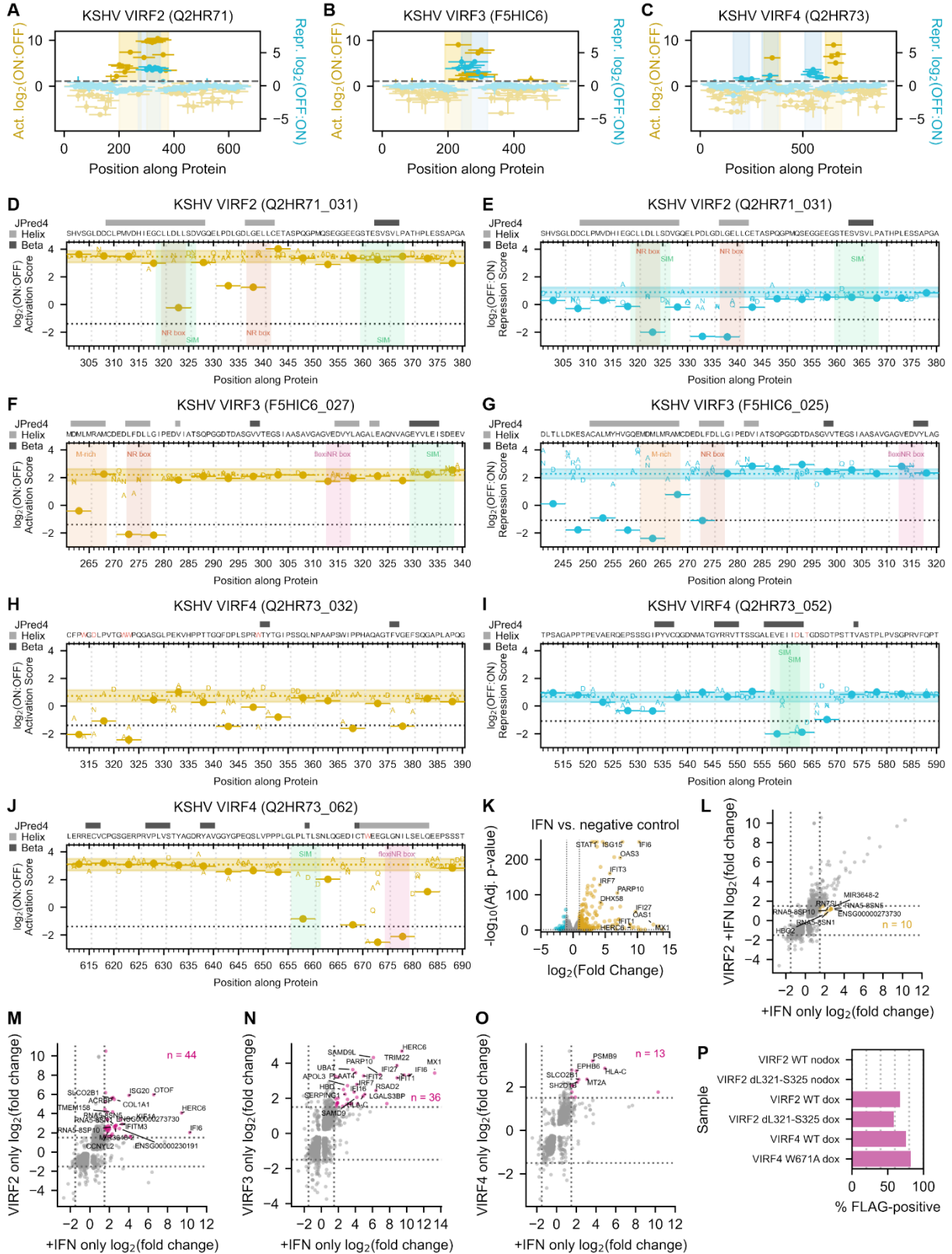


Fig. S6 | Identification of effector domains and essential amino acids in VIRF proteins, related to Figure 5. (A-C) Tiling plots of VIRF2 (A), VIRF3 (B), and VIRF4 (C), highlighting their activation (yellow), repression (blue), and dual (overlap of yellow and blue) effector domains. (D-E) Perturbation plots of the dual effector domain in VIRF2, showing the effects of 5aa deletions and single-residue substitutions on activation (D) and repression (E). Motifs are highlighted with a colored vertical span and indicated on the plot. (F-G) Perturbation plots of the dual effector domain in VIRF3, showing the effects on activation (F) and repression (G). (H-J) Perturbation plots of the dual effector domain (H, only activation shown), moderate-strength repression domain (I), and strong activation domain (J) in VIRF4. (K) Volcano plot from RNA-seq differential expression analysis comparing gene expression profiles under 24 hours of interferon (IFN) beta treatment versus 48 hours of overexpression of mCitrine, a negative control that does not change host gene expression. The plot shows significantly upregulated (yellow) and downregulated (blue) genes, with many well-described interferon-stimulated genes (a subset is labeled) upregulated after IFN-beta treatment. (L-O) Scatter plots comparing how the same gene changes under various conditions versus under IFN-beta treatment alone from (K), with the x- and y-axes showing the log₂ fold changes in gene expression in each condition relative to the mCitrine negative control. These comparisons involve VIRF2 overexpression with IFN-beta treatment versus IFN-beta treatment alone (L), VIRF2 overexpression alone versus IFN-beta treatment alone (M), VIRF3 overexpression alone versus IFN-beta treatment alone (N), and VIRF4 overexpression alone versus IFN-beta treatment alone (O). Genes are filtered by adjusted p-value (<0.05), and dashed lines are set at log₂ fold changes of -1.5 and 1.5. (P) These comparisons include Summary of 3xFLAG-tagged WT and mutant VIRF protein levels as estimated using anti-FLAG staining and flow cytometry. A dox-inducible promoter (minCMV driven by rTetR-VP48) is used to induce expression of the 3xFLAG-tagged full-length proteins indicated on the y-axes (See Fig. 6F, and Methods). Mutants: VIRF2 with deletion of L321 to S325 (dL321-S325) and VIRF4 with substitution of tryptophan 671 with alanine (W671A).

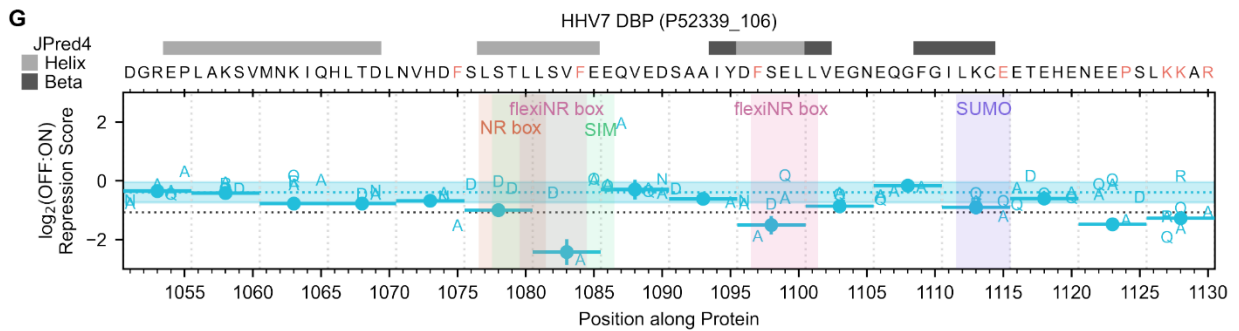
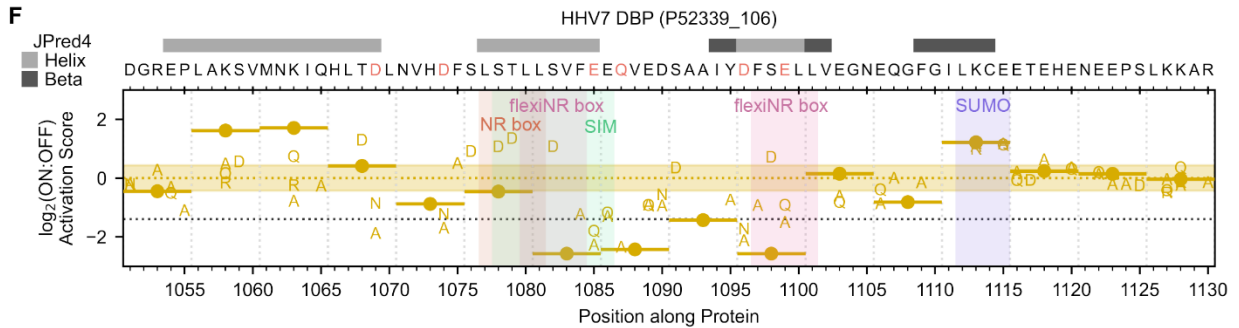
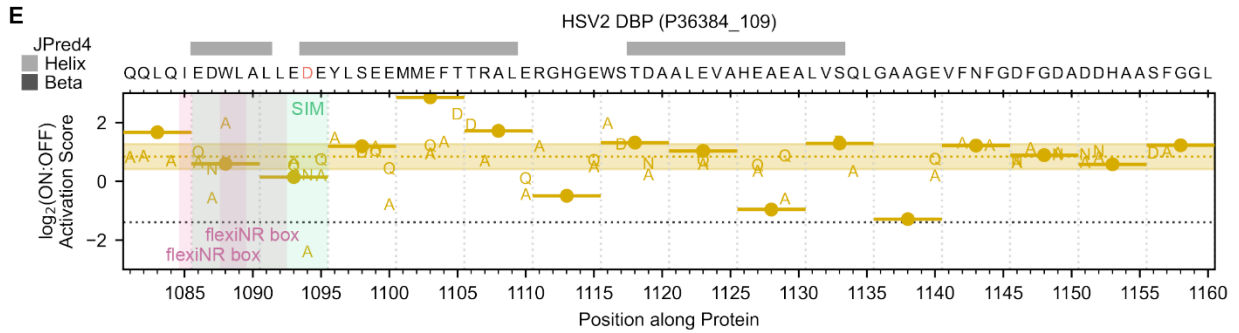
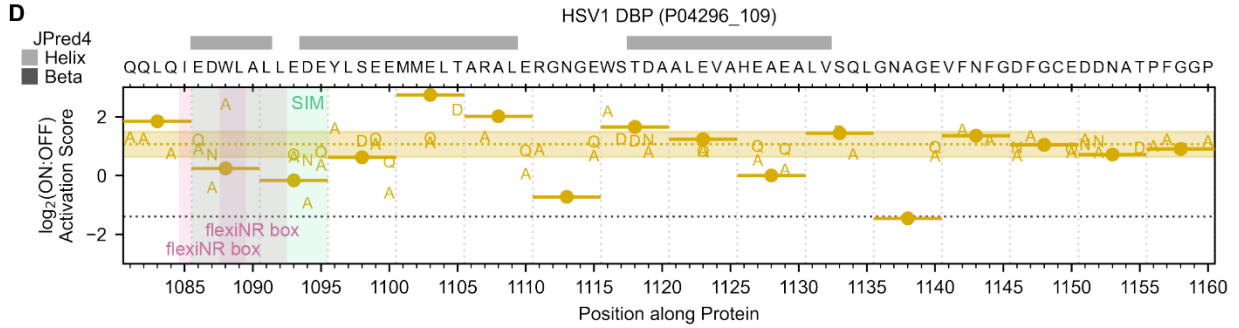
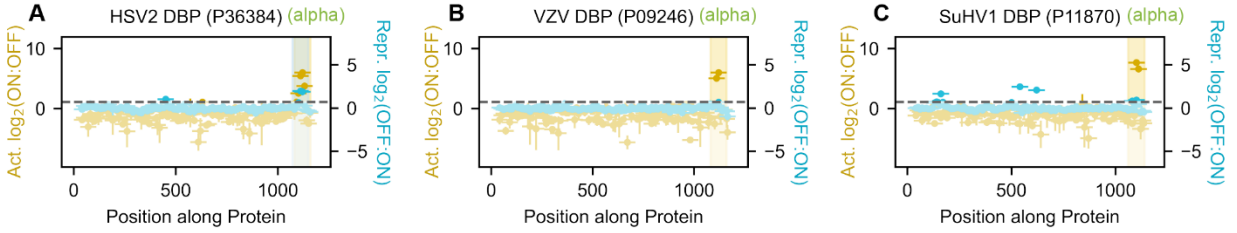


Fig. S7 | DBP domains and perturbation analysis, related to Figure 6. (A-C) Tiling plots of three alphaherpesvirus DBP homologs showing their C-terminal activation domains, which, in the case of HSV2 (A), also has repression potential. **(D-G)** Perturbation plots showing the effects of 5aa deletions and single-residue substitutions on activation (D-F) or repression (G) by various DBP homologs.